J. Cell. Mol. Med. Vol 13, No 9B, 2009 pp. 3730-3741

Embryonic stem cell-derived cardiomyocytes as a model to study fetal arrhythmia related to maternal disease

Siti H. Sheikh Abdul Kadir [a, b, c], Nadire N. Ali [a], Maxime Mioulane [a], Marta Brito-Martins [a], Shadi Abu-Hayyeh [a], Gabor Foldes [a], Alexey V. Moshkov [a], Catherine Williamson [b], Sian E. Harding [a], Julia Gorelik [a, *]

[a] *National Heart and Lung Institute, Imperial College London, London, UK*
[b] *Institute of Reproductive and Developmental Biology, Imperial College London, Hammersmith Campus, London, UK*
[c] *Faculty of Medicine, Universiti Teknologi MARA, Selangor, Malaysia*

Received: October 28, 2008; Accepted: February 23, 2009

Abstract

Embryonic stem cell-derived cardiomyocytes (ESC-CM) have many of the phenotypic properties of authentic cardiomyocytes, and great interest has been shown in their possibilities for modelling human disease. Obstetric cholestasis affects 1 in 200 pregnant women in the United Kingdom. It is characterized by raised serum bile acids and complicated by premature delivery and unexplained fetal death at late gestation. It has been suggested that the fetal death is caused by the enhanced arrhythmogenic effect of bile acids in the fetal heart, and shown that neonatal susceptibility to bile acid-induced arrhythmia is lost in the adult rat cardiomyocyte. However, the mechanisms of the observed bile acid effects are not fully understood and their *in vivo* study in human beings is difficult. Here we use ESC-CM from both human and mouse ESCs to test our proposal that immature cardiomyocytes are more susceptible to the effect of raised bile acids than mature ones. We show that early ESC-CM exhibit bile acid-induced disruption of rhythm, depression of contraction and desynchronization of cell coupling. In both species the ESC-CM become resistant to these arrhythmias as the cells mature, and this develops in line with the respective gestational periods of mouse and human. This represents the first demonstration of the use of ESC-CM as a model system for human cardiac pathology, and opens the way for both investigation of mechanisms and a high throughput screen for drug discovery.

Keywords: embryonic stem cell-derived cardiomyocytes (ESC-CM) • obstetric cholestasis • bile acids • arrhythmias

Introduction

The discovery of embryonic stem cells (ESCs), and the observation that they can be differentiated into cardiac myocytes with the appropriate electrical, contractile and signalling properties [1–5] has raised great expectations in the cardiac research community. The most obvious use for these ESC-derived cardiomyocytes (ESC-CM) is in cardiac repair [6, 7] but, among the cell sources considered for this task, they have arguably the greatest barriers to clinical application [8, 9]. A more readily achievable use that has been proposed is as a model system for the cardiac researcher [3].

*Correspondence to: Dr Julia GORELIK,
Imperial College London, National Heart and Lung Institute,
Guy Scadding Building, Dovehouse Street, London SW3 6LY, UK.
Tel.: 44(0)207 352 8121 ext. 3324
Fax: 44(0)207 823 3392
E-mail: j.gorelik@imperial.ac.uk

Primary adult myocytes are stable in culture for only a few days [10, 11], fetal/neonatal myocytes will be usable for weeks but are only obtained from rodent, and cardiac cell lines with stable contractile activity are rare and again of rodent origin. Maintenance of contracting human ESC-CM has been observed for over 7 months, the longest period examined so far in our own laboratory. Furthermore, we and others have also shown their maturation in terms of morphology, membrane currents and excitation–contraction coupling [12, 13]. The prospect of a cardiac cell of human origin, with a survival in culture over timescales of months, has opened up possibilities for investigation of mechanisms of cardiac development and cardiac pathology, as well as uses in drug discovery and toxicology.

To realize this potential, however, detailed investigations must be made on the characteristics of the ESC-CM and the nature of their development in culture. It might be predicted that the most amenable pathological conditions for ESC-CM as a model system

doi:10.1111/j.1582-4934.2009.00741.x

would be those that occur in fetal life. In this study, we have investigated both human and mouse ESC-CM as a potential model system for intrauterine fetal death in obstetric cholestasis (OC). This is a liver disease of pregnancy characterized by raised serum bile acids. It can be complicated by fetal distress, intrauterine death and pre-term labour [14–16]. OC is common, affecting 1 in 200 pregnancies in the United Kingdom [17]. The aetiology of the fetal death is poorly understood. It is thought to occur suddenly, as there is no evidence of preceding utero-placental insufficiency and the fetal autopsy is normal [18]. It has been suggested as arrhythmic, because placental histology shows non-specific changes consistent with hypoxia [19] and an abnormal fetal heart rate ($\leq$100 or $\geq$180 beats/min.) has been observed [15, 20–22]. In addition the presence of neonatal cholestasis causes persistence of arrhythmias in the neonatal period following identification of conduction abnormalities *in utero* [23]. The principal maternal bile acids that are raised in OC are cholic acid and chenodeoxycholic acid, and these become tauro-conjugated. Cholic acid is the most sensitive bile acid for early diagnosis and follow-up of OC, and can rise as much as 100-fold. Fetal complications occur more commonly when the maternal total bile acid level is $>$40 μmol/l [21, 24]. Experiments on human fetal myocytes are clearly difficult for ethical and logistic reasons. We have previously demonstrated that tauro-cholate (TC) can acutely alter the rate, rhythm and intercellular coupling of cardiomyocyte contraction and Ca^{2+} transients, using an *in vitro* model of 1–2-day-old neonatal rat cardiomyocytes [25, 26]. Adult rat myocytes, in contrast, were relatively resistant to TC, which would be consistent with differential sensitivities of the maternal and fetal hearts and with the observation that women with OC have not been reported to suffer from cardiac conduction abnormalities.

In the present paper, we follow the sensitivity of ESC-CM during maturation over 25 days (mouse) and 72 days (human), and compare the human ESC-CM with adult human ventricular myocytes. We show contraction changes and arrhythmia generation with TC in early stage human or mouse ESC-CM which parallel our previous results with regard to their nature and underlying Ca^{2+} dynamics. We find clear changes in sensitivity to TC with maturation over appropriate time scales in the two species, so that late stage human ESC-CM have susceptibilities similar to those of the adult myocytes. This represents the first demonstration of the use of ESC-CM as a model system for human cardiac pathology, and opens the way for both investigation of mechanisms and a high throughput screen for drug discovery.

Materials and methods

Chemicals

All chemicals were purchased from Gibco/Invitrogen (Paisley, Scotland), unless otherwise stated. Nunc Petri dishes and tissue culture plastic were from Fisher Scientific UK (Loughborough, UK).

Mouse embryonic stem cell cultures and differentiation into cardiomyocytes

Two mouse ESC lines were used: The feeder cell-dependent D3 line (ATCC), propagated on a confluent layer of mitomycin C-treated, mitotically inactive SNL feeder fibroblasts (iSNL), and the feeder-independent E14Tg2a (obtained from Austin Smith, Cambridge, UK). These were cultured in high (4.5 g/l) glucose Dulbecco's modified Eagle's medium (KO-DMEM), supplemented with 15% knockout serum replacement (KOSR) (D3 line) or 15% batch-tested fetal calf serum (E14Tg2a), 2 mM L-glutamax, 1% non-essential amino acids (100$\times$ stock), 50 U/ml penicillin, 50 μg/ml streptomycin, 0.1 mM β-mercaptoethanol (Sigma) and 1000 U/ml leukaemia inhibitory factor (LIF; ESGRO-LIF, Chemicon, Harrow, UK). Both lines were induced to differentiate in this medium without LIF; the supplements KOSR and FCS used during propagation were also replaced with a batch-tested 15% FCS that gave beating embryoid bodies (EBs) of up to 96%. Differentiation was induced via EBs in hanging drops (400 cells / 20 μl) for 2 days, followed by 3–5 days of culture in Petri dishes (approx. 50–60 EBs/6-mm dish/ 5 ml) and then plating out onto 0.1% gelatinized glass cover slips (1–3 EBs/cover slip). Spontaneously beating ESC-CM from both lines appeared in EB outgrowths generally at around day 7 onwards and continued beating for approximately 21 days. During this time period, cover slips corresponding to 'early' (day 7–10), 'intermediate' (day 12–14) and 'late' (day 15–25) cardiac differentiation stages (classification by Boheler) [27] were transferred to the stage of the scanning ion conductance microscope (SICM) for observation. ESC-CM from E14Tg2a were studied at 11–14 and 29–30 days following induction of differentiation.

Human ESC cultures and differentiation into cardiomyocytes

Human ESC (H7 line) was supplied by Geron Corporation (Menlo Park, CA, USA). Cells were cultured on Matrigel-coated six-well plates in mouse embryonic fibroblast-conditioned medium (MEF-CM), supplemented by 8 ng/ml recombinant human bFGF and antibiotics (50 U/ml penicillin and 50 μl/ml streptomycin).

All procedures for producing MEF-CM in the presence of 4 ng/ml bFGF, the sub-culturing of the H7 cells and their differentiation *via* EBs were as described by Geron (http://www.geron.com/PDF/scprotocols.pdf), with the exception that mitomycin C was used for mitotic inactivation of the MEFs instead of irradiation. After 4 days, EBs of varying sizes were plated out onto 0.5% gelatine-coated glass or plastic and studied at time periods from days 9–12 of differentiation onwards as spontaneously beating myocytes appeared from this time.

Isolation and contraction measurement of adult ventricular cardiomyocytes

Ventricular myocytes were isolated from myocardium of explanted failing human hearts as previously described [28]. Cells were placed in a bath on the stage of an inverted microscope and superfused with oxygenated Krebs-Henseleit buffer (mM: NaCl 119.10, KCl 4.70, $MgSO_4$ 0.94, KH_2PO_4 1.20, $NaHCO_3$ 25.00, glucose 11.5, $CaCl_2$ 4.0, pH 7.4) at 32 $\pm$ 0.5°C. Cells were paced electrically using a biphasic 50 V pulse at 0.2 Hz. Contraction amplitude of myocytes was measured via a video camera using software

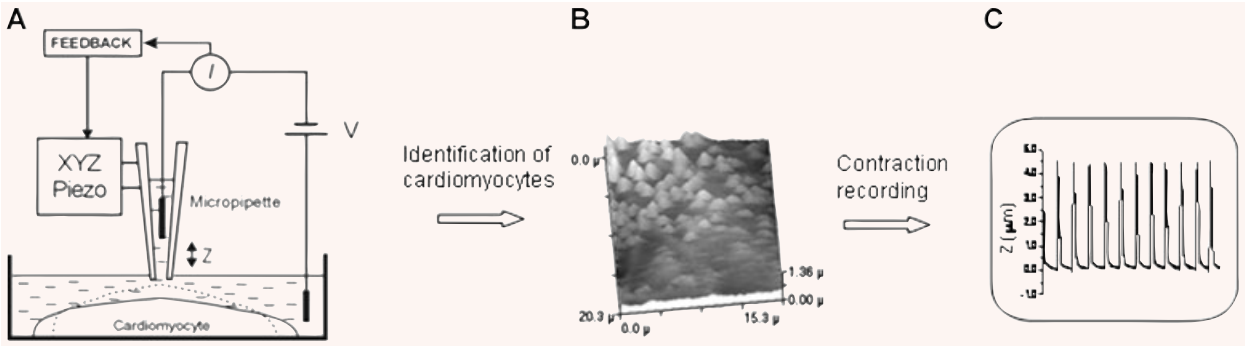

Fig. 1 (**A**) Schematic diagram of the scanning ion conductance microscopy (SICM). The SICM consists of a glass micropipette probe filled with physiological medium lowered into a bath toward the cell surface, which represents an insulating barrier for ions. As the tip of the micropipette approaches the cell membrane, the ion conductance reduces because the gap that ions can flow through is decreased. Changes of the ion current (I_{ion}) are monitored by a current amplifier, and the amplifier output is used by the microscope control unit as a feedback signal to keep the separation distance between the electrode tip and sample constant by applying appropriate voltages to the *Z*-piezo drive. The *XY*-piezo scanner performs raster scanning while the feedback control system maintains constant separation distance. Therefore, the path of the tip follows the profile of the cell surface resulting in the generation of a topographical image. (**B**) Topographical SICM image of the surface of mESC-CM. Identification of a contracting cell in a culture of mESC-CM by SICM. The light peaks are due to the surface rise of a contracting cell. (**C**) Recording of the vertical displacement of the cell surface of a cardiomyocyte during contraction.

from IonOptix (London, UK). Once tracking was established on a suitable cell, a minimum of 10 min. was allowed to elapse before beginning an experiment, to ensure that the contraction amplitude (% shortening) was stable and that the relaxed length of the cell was not altering with time. Concentrations of TC were applied for 10 min., and wash periods were >20 min.

Effect of TC on the amplitude and rhythm of contraction of ESC-CM

Topographic imaging of the cells is performed with SICM methods [29]. Briefly, the pipette mounted on a piezo stage is moved over the cell while maintaining a fixed distance from the surface. (Fig. 1A) This is achieved by a feedback control keeping the ion current through the pipette constant. Firstly, we performed imaging of various ESC-CM layer zones and identified contracting cardiomyocytes [30] (Fig. 1B). To investigate the changes of the rhythm of cardiomyocyte contraction caused by the addition of bile acids, we recorded the vertical cell displacement of individual cells as described previously [31]. As the cell surface rises during contraction, the micropipette is displaced vertically. The measurement allows alterations in contraction to be recorded (Fig. 1C).

Calcium dynamics

The cells were loaded with fluo-4 acetoxymethylester (fluo-4 AM; Molecular Probes, Eugene, OR, USA) in a medium containing a mixture of part Leibovitz's L-15 (Gibco) and part Hanks' balanced salt solution buffer (Gibco) at room temperature for 45 min. Cells were rewashed five times with the medium, followed by a post-incubation period of 20 min. to allow for complete intracellular dye cleavage [32]. Ca^{2+} fluctuations were imaged by exciting fluo-4 at 450–480 nm and detecting emitted fluorescence at >520 nm using an intensified CoolView IDI camera system (CCD, Photonic Science, Sussex, UK) coupled to a Nikon TE-2000 inverted microscope (Kingston upon Thames, UK) and controlled by Image-Pro Plus software (Media Cybernetics, Wokingham, UK).

Immunocytochemistry

Cell were fixed with 4% paraformaldehyde, permeabilized with 0.2% Triton X-100, and labelled with anti-cardiac specific troponin I (Santa Cruz, 1:200 dilution, Santa Cruz, CA, USA), anti-Ki67 (proliferation marker, Abcam, 1:100) and anti-myosin heavy chain α/β (MHC-α/β, Abcam, 1:200) primary antibodies. Primary antibodies were detected with FITC (Abcam), Alexa 488 (Invitrogen), Alexa 546 (Invitrogen) and Cy5 (Abcam, Cambridge, MA, USA) conjugated secondary antibodies (all 1:400). DNA was visualized with DAPI (0.5 µg/ml; Sigma). Images were acquired on Zeiss Axio Observer Z1 fluorescence microscopy (Welwyn Garden City, UK).

Statistics

Results were expressed as mean and standard error or standard deviation (S.D.). Comparisons were made using the unpaired t-test. The data were checked for normal distribution prior to parametric analyses.

Results

We compared the effect of TC on the contraction of mESC-CM at three different stages of differentiation according to the Boheler classification [27]. Figure 2 shows typical examples of the influence of different concentrations of TC on the rhythm and amplitude of contraction of mESC-CM.

Table 1 Effect of 0.1 mM and 1.0 mM TC on amplitude and rhythm of hESC-CM between 13 days and 71 days of differentiation

Day of development	Effect of bile acid			
	TC 0.1 mM		TC 1 mM	
	Amplitude	Rhythm	Amplitude	Rhythm
13	Effect	Effect	Effect	Effect
13	No effect	Effect	Effect	Effect
13	Effect	Effect	Effect	Effect
18	No effect	Effect	Effect	Effect
18	No effect	Effect	Effect	Effect
19	No effect	Effect	Effect	Effect
19	Effect	Effect	Effect	Effect
24	No effect	Effect	Effect	Effect
28	Effect	Effect	Effect	Effect
28	Effect	Effect	Effect	Effect
28	Effect	Effect	Effect	Effect
29	No effect	Effect	Effect	Effect
29	No effect	Effect	Effect	Effect
42	No effect	No effect	No effect	Effect
43	No effect	No effect	No effect	Effect
43	No effect	No effect	No effect	Effect
43	No effect	No effect	No effect	Effect
48	Effect	No effect	Effect	Effect
54	No effect	No effect	No effect	No effect
60	No effect	No effect	No effect	No effect
60	No effect	No effect	No effect	No effect
71	No effect	No effect	No effect	No effect
71	No effect	No effect	No effect	No effect
71	No effect	No effect	No effect	Effect

mESC-CM: early stage

Prior to the addition of TC the cells contracted spontaneously and rhythmically at a rate of 29.0 $\pm$ 1.7 beats per min. (bpm, mean $\pm$ S.D., $n = 6$) with an amplitude of 100%. When 0.1 mM TC was added to the culture medium of these cells there was an overall reduction both in the rate and amplitude of contraction (Fig. 3). The rate of contraction was reduced to 21.5 $\pm$ 1.6 bpm, (mean $\pm$ S.D., $n = 6$. $P < 0.001$) and amplitude of contraction decreased to 71.8% $\pm$ 19.4% of control ($P < 0.05$). Addition of 1 mM TC resulted in further reductions in the rate to 11.6 $\pm$ 1.6 bpm ($P < 0.001$) and amplitude of contraction (38.5% $\pm$ 5.3% of control, $P < 0.05$).

mESC-CM: intermediate stage

The initial rate of contraction was 36.3 $\pm$ 1.9 bpm ($n = 7$) (Fig. 2B). Addition of 0.1 mM TC again caused a reduction in both the rate and the amplitude of contraction. The rate decreased to 29.7 $\pm$3.6, $P < 0.05$, while the amplitude was reduced from 100% to 64.9% $\pm$ 22.6%, $P < 0.05$ ($n = 7$). Addition of 1.0 mM

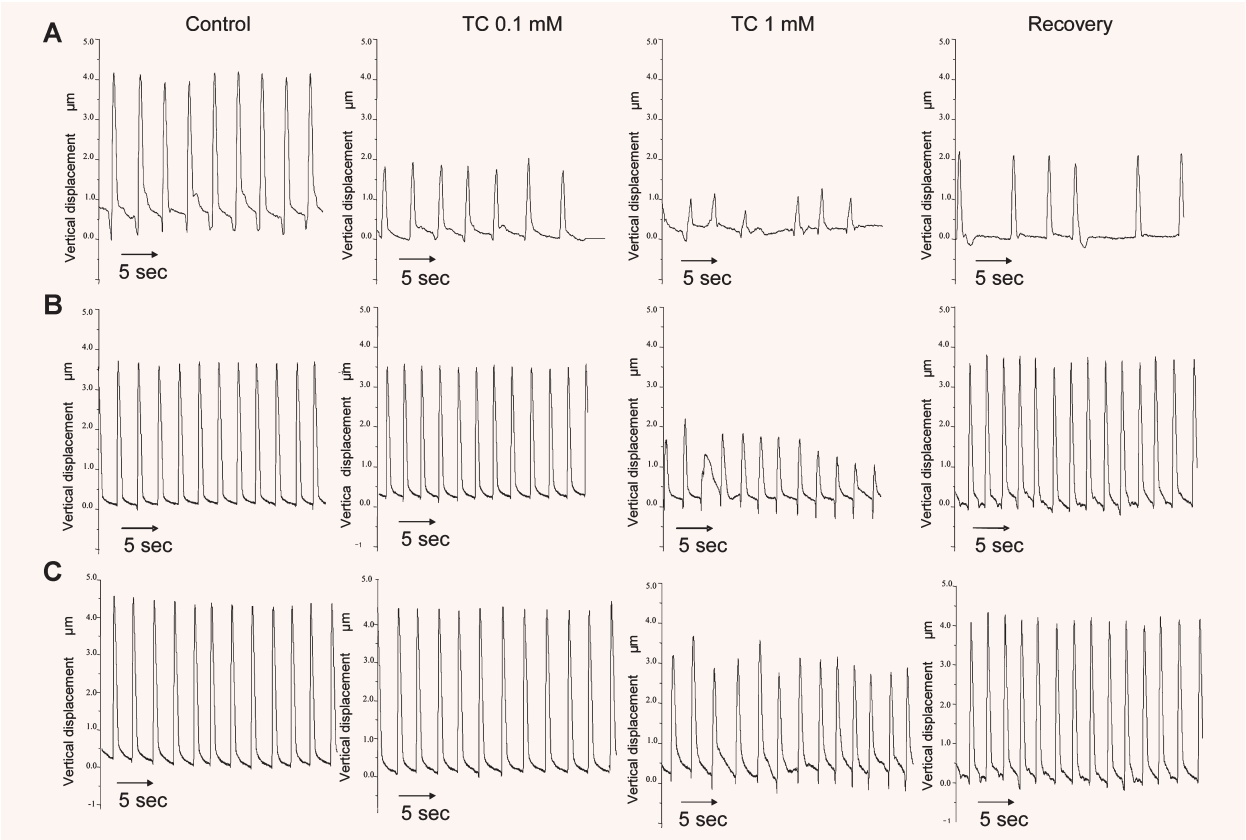

Fig. 2 Measurement of contraction of mESC-CM in the different stages of differentiation. Representative traces of the influence of addition of 0.1 mM and 1.0 mM TC on the rate and amplitude of contraction of mESC-CM in the early (**A**), intermediate (**B**) and late (**C**) stages of differentiation.

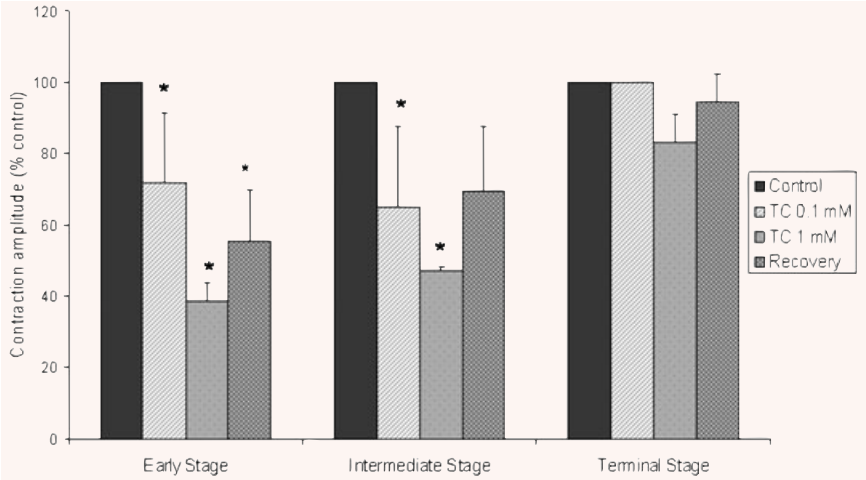

Fig. 3 Graph demonstrating the influence of adding 0.1 mM and 1.0 mM TC on the amplitude of contraction in mESC-CM at the early, intermediate and terminal stages of differentiation. This is represented as a percentage (%) of the amplitude of contraction in cells prior to the addition of TC (designated controls). The extent to which the amplitude of contraction returns to normal after transfer of cells into TC-free medium is also shown. (*Control *versus* $P < 0.05$). ($n = 6$ early stage; $n = 7$ intermediate stage; $n = 5$ terminal stage.)

TC caused further reductions in these parameters, rate decreasing to 7.1 $\pm$ 5.4, $P < 0.001$ and the amplitude to 47.1% $\pm$ 0.9% of control values. Although there was an increase in the rate of contraction following transfer to TC-free medium (26.3 $\pm$ 4.2; $P < 0.05$), this remained lower than control, as did amplitude of contraction (Fig. 3). Rhythm disturbances were observed at both 0.1 and 1 mM TC, but showed both faster and slower components compared to untreated cells (Fig. 4B).

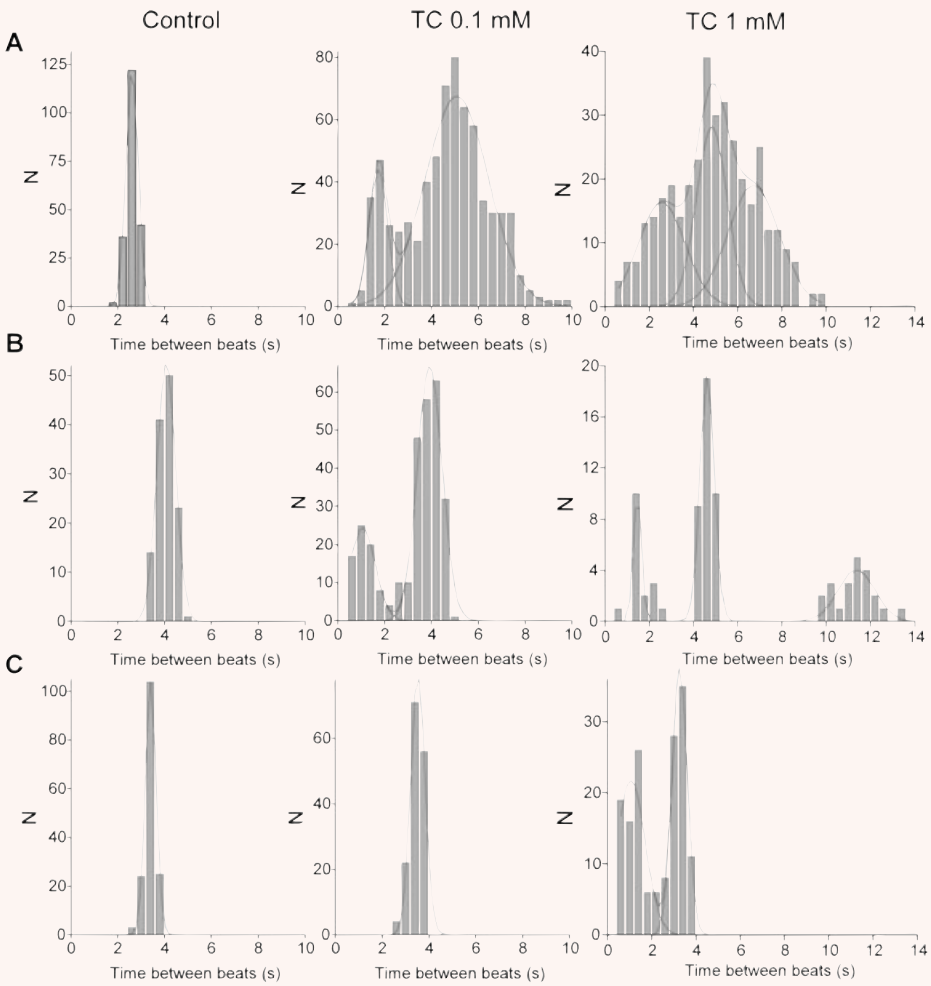

Fig. 4 (**A**) Representative histogram of the interval of time between beats of mESC-CM in the early stage of differentiation. (**B**) Representative histogram of the interval of time between beats of mESC-CM in the intermediate stage of differentiation. (**C**) Representative histogram of the interval of time between beats of mESC-CM in the terminal stage of differentiation.

mESC-CM: terminal stage

Initial rate was 33.0 ± 2.0 bpm, $n = 5$ (mean ± S.D.). Addition of 0.1 mM TC had no effect on rate 33.8 ± 1.6, amplitude (Fig. 3) or rhythm (Fig. 4). With 1.0 mM TC, rate was decreased to 28.6 ± 2.7 bpm, $P < 0.05$ but amplitude was not significantly altered (Fig. 3). Rhythm disturbances were noted at this concentration, with a faster component added to the main distribution indicating ectopic beats with a stable rhythm (Fig. 4C). Changes were fully reversible following transfer to TC-free medium.

ESC-CM from the E14Tg2a line [33, 34] showed similar arrhythmias in early stage of differentiation to those from D3, with five of six clusters showing disruption of rhythm or amplitude following addition of 0.1 mM to 1 mM TC to the culture medium. We showed that in the late stage of differentiation (29–30 days) the amplitude of contraction was not significantly changed even after 1 mM TC compare with the early stage of differentiation. (Supporting Information, Fig. 1).

Calcium transient dynamics

Example frames from recordings (Supporting Information, Movie S1) of intracellular Ca^{2+} dynamics of mESC-CM (intermediate stage) after loading with Fluo-4 are shown in Fig. 5. Standard bright-field microscopy revealed synchronous rhythmic contraction of the network of cells, and this was confirmed by the synchronous Ca^{2+} transients throughout the cluster (Fig. 5, left

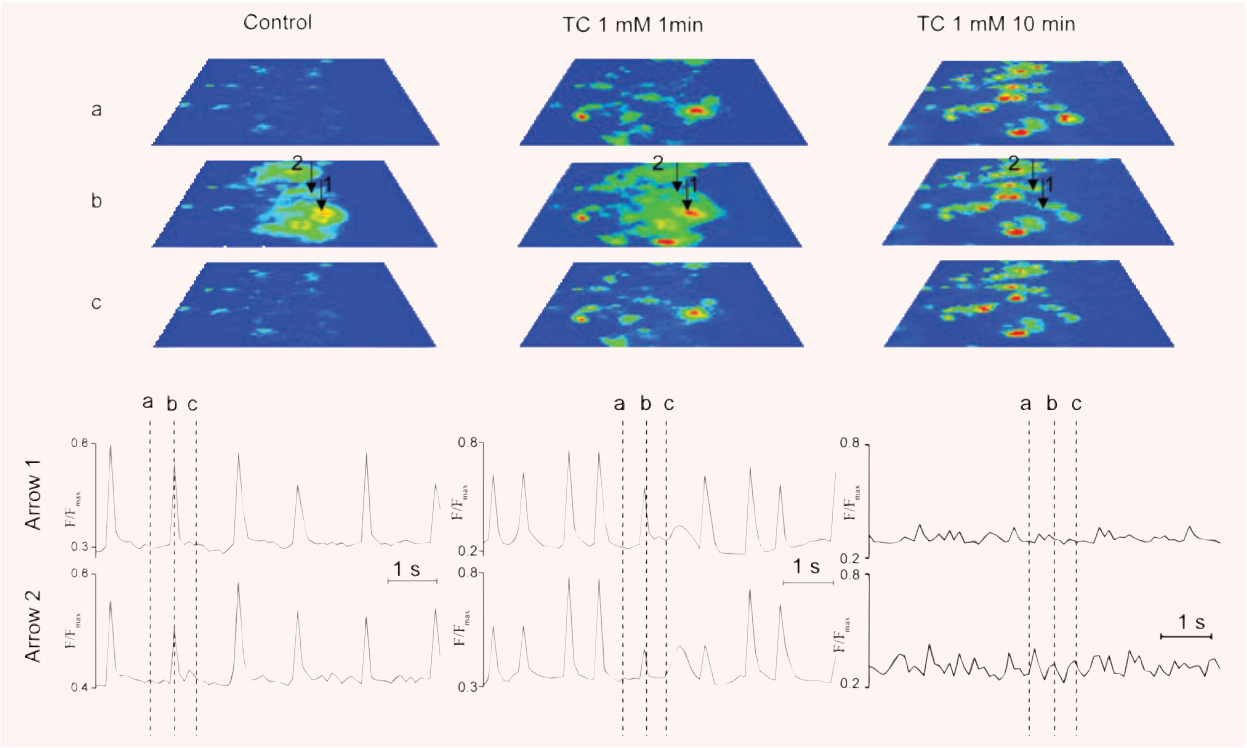

Fig. 5 Intracellular Ca^{2+} dynamics of mESC-CM after loading with Fluo-4. The left hand panel represents the contraction of mESC-CM loaded with Fluo-4 before addition of TC to the culture medium. The images are taken at time-points before (**A**), at the peak of (**B**) and after (**C**) the calcium transient. The central panel shows contraction following addition of 1 mM TC to the culture medium. The right hand panel demonstrates the alterations in calcium transients that were observed after 10 min. treatment with 1 mM TC. Transient recordings at the points indicated by the two arrows are shown.

column of images). Transient recordings at the points indicated by the two arrows are shown in the tracings below. Fluorescent images of time-points before (A), at the peak of (B) and after (C) the calcium transient are shown, and indicated on the tracings. When TC was added to the mESC-CM (Fig. 5, central panel) signs of Ca^{2+} overload were seen in diastole, and rhythm disturbances described above were reflected in the timing of the Ca^{2+} transients. After 10 min. treatment with 1 mM TC, this preparation showed markedly raised Ca^{2+} in diastole and a marked reduction in Ca^{2+} transient amplitude in systole (Fig. 5, right column of images). Synchronized contraction could no longer be observed (Supporting Information, Movie S1).

hESC-CM: early *versus* late stages

hESC-CM were compared at early (<30 days) and late (>30 days) stages of differentiation. Addition of 0.1 mM TC at the early stage of differentiation caused a change in rate from 23.2 ± 4.8 bpm (mean ± S.D.) to 16.3 ± 1.6 bpm, $n = 10$, $P < 0.05$ and the amplitude of contraction was reduced to 88.1 ± 7.0% of control (non-significant change) (mean ± S.D.) (Fig. 6A). Addition of 1.0 mM TC reduced these parameters further to 7.4 ± 2.7 bpm, and 57.9% ± 8.0%, $n = 6$, $P < 0.001$, respectively (Fig. 6B). The amplitude of contraction recovered slightly to 63.3% ± 4.0% following transfer of cells to TC-free medium which is not significant. In hESC-CM at the late stage of differentiation, addition of 0.1 mM or 1 mM TC did not significantly influence the amplitude and rate of contraction. Interbeat interval for experiments where arrhythmias were detected is shown in Fig. 7. When 0.1 mM TC was added to hESC-CM in the early stage of differentiation there were two peaks on the histogram consistent with bigeminy (Fig. 7A, middle graph). After addition of 1.0 mM TC the histogram remained abnormal and the bigeminy was more marked (Fig. 7A, right graph). Addition of 0.1 mM TC to hESCM at the terminal stage of differentiation did not affect beat-to-beat interval. Table 1 shows hESC-CM at different stages of differentiation. In hESC-CM at 13–29 days even 0.1 mM TC caused abnormal amplitude of contraction in 4 out of 10 cultures and abnormal rhythm in all cultures. Higher dose of TC (1 mM) affected all cultures. At the later stages rhythm of contraction was influenced only by 1 mM TC in 6 out of 11 preparations.

The hESC-CM isolated from EBs were stained positive for sarcomeric proteins typical of myocytes, such as MHC-α/β and cardiac troponin I. Many hESC-CM retain their immature structural characteristics with an irregular myofibrillar distribution, but hESC-CM

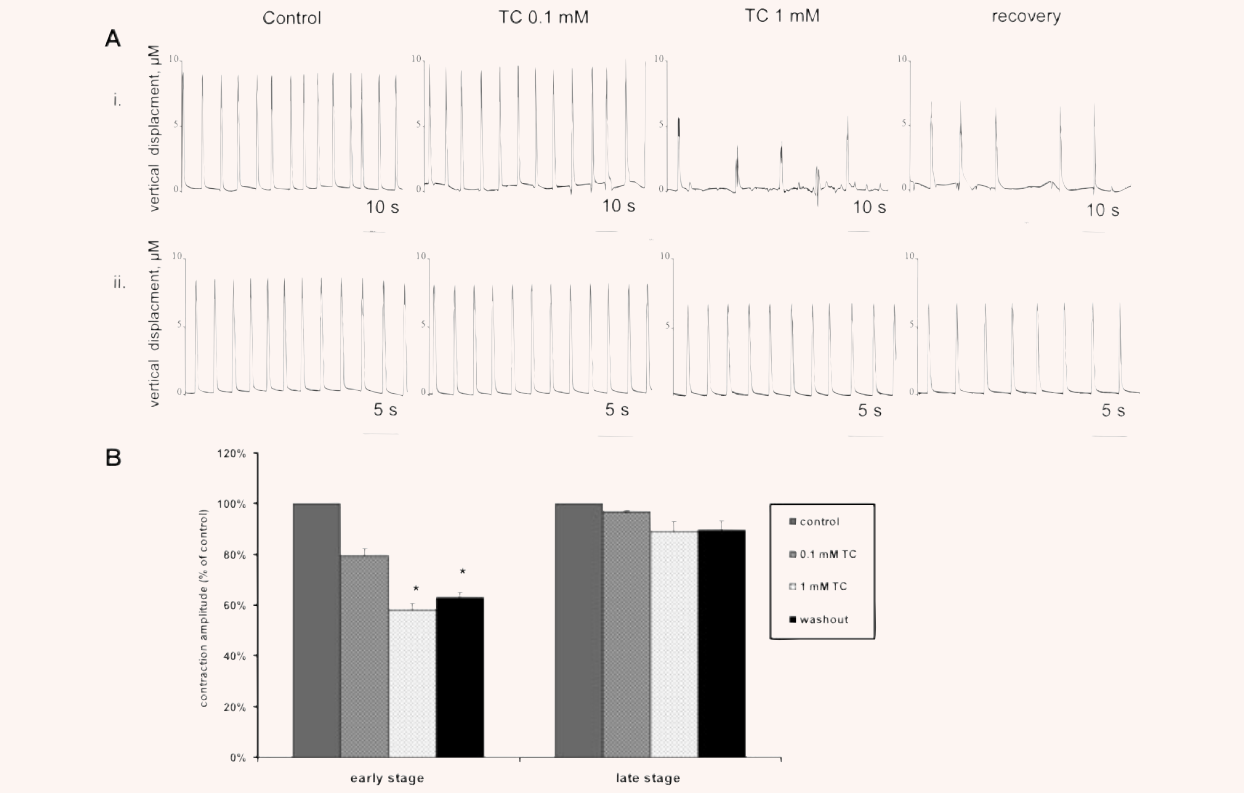

Fig. 6 (**A**) Example traces for hESC-CM at different stages of differentiation, (*i*) <30 days of differentiation and (*ii*) >30 days of differentiation following addition of TC and also after 1 hour of recovery in TC-free medium. (**B**) Averaged data for influence of addition of 0.1 mM and 1.0 mM TC on the amplitude of contraction in hESC-CM at the early and late stages of differentiation. This is represented as a percentage (%) of the amplitude of contraction in cells prior to the addition of TC (designated controls). The extent to which the amplitude of contraction returns to normal after transfer to TC-free medium is also shown. (*Control *versus* $P < 0.001$; $n = 10$ – early stage; $n = 11$ – late stage.)

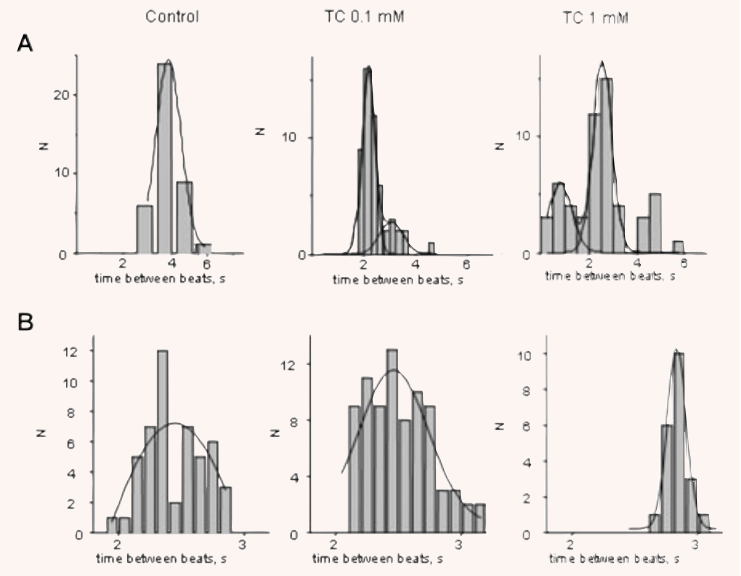

Fig. 7 Representative histogram of the interval of time between beats of hESC-CM (**A**) in the early stage of differentiation and (**B**) in the late stage of differentiation.

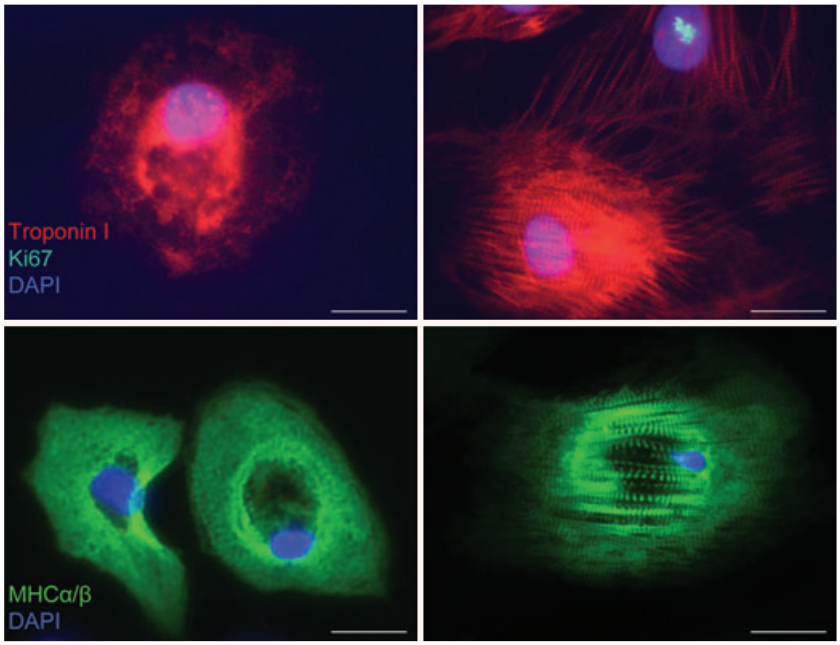

Fig. 8 Representative immunofluorescence images showing hESC-CM stained positive for the markers cardiac specific troponin I (red) and myosin heavy chain α/β (MHC-α/β, green) from hESC-CM (left panel) in immature stage of differentiation and (right panel) in the mature stage of differentiation. Mitotic marker Ki67 shows nuclear expression in proliferating cell (green, nuclear spotted pattern). The striations characteristic of the sarcomeric structures in hESC-CM can be seen. DAPI (blue) was used for nuclear staining. Scale bar, 20 μm.

with a highly organized sarcomeric pattern can be found from both immature (Fig. 8, left panel) and mature cultures (Fig. 8, right panel).

The influence of TC was also studied in human adult ventricular cardiomyocytes. Rhythm was maintained in the paced cardiomyocytes, and there was no significant effect on contraction amplitude, time-to-peak contraction or time-to-50% or 90% relaxation following treatment with 0.1 mM to 1 mM TC (Fig. 9). However addition of 3 mM TC to the culture medium caused arrhythmia (Fig. 9A).

Discussion

We have demonstrated that TC induced arrhythmias can be observed at early stages of differentiation in mESC-CM and hESC-CM. The main characteristics of the arrhythmia were the reduction of the rate of contraction, depression of amplitude of contraction, irregularity of beating, calcium overload and disorganization of the synchronously beating network of cardiomyocytes. In both mESC-CM and hESC-CM this susceptibility was lost with increasing time in culture, and the difference in the rate at which this occurred was consistent with the relative gestational periods in the two species. Finally, the hESC-CM at around 60 days were almost completely resistant to TC, and similar to adult human ventricular myocytes in their response. These results parallel our previous findings that rat neonatal cardiomyocytes are more susceptible to bile acid-induced arrhythmias than adult [25], and supports the hypothesis that fetal death in OC is caused by differential sensitivity of the fetal myocardium to bile acid-induced arrhythmia compared to the adult maternal heart [35].

Maturity in ESC-CM is an area of intense investigation, and encompasses a number of aspects. During the early stages of mESC-CM differentiation, the bundles of myofibrils lack visible organization. At the intermediate stage of differentiation mESC-CM are characterized by well developed myofibrils and sarcomeres with cell–cell junctions consistent with those observed in cardiomyocytes developing in the heart. During the terminal stage of differentiation well-organized bundles of myofibrils, sarcomeres and gap junctions can be observed [27]. Human ESC-CM at an early stage of differentiation lack organized myofibrils, a morphology that resembles early fetal cardiomyocytes. In contrast, mature hESC-CM differentiated for 60 days or more possess myofibrils that have an organized appearance and sarcomeres that resemble the adult phenotype [12, 36]. Loss of proliferative activity is also a marker of progression away from the immature phenotype, and occurs over a similar time period of around 60 days for hESC-CM. Decreased proliferation may be complementary to sarcomeric organization because disassembly of sarcomeres is necessary for cytokinesis [32, 37].

However, it is well known that immature myocytes are strongly influenced by physical cues such as stretch to stimulate sarcomere alignment. Without such mechanical patterning, it is not surprising that alignment of sarcomeres is a relatively slow process in cultured ESC-CM. More pertinent to assessment of maturity, particularly in the context of studying the arrhythmic potential of interventions, is the development of the adult phenotype in terms of ion currents and intracellular calcium handling. In these respects, hESC-CM show convincing progress towards the adult phenotype. Repolarization currents such as I_{to1} and I_{Kl} develop after 55 days in culture, while I_f decreases [13, 32] with I_{Kr} and I_{CaL}

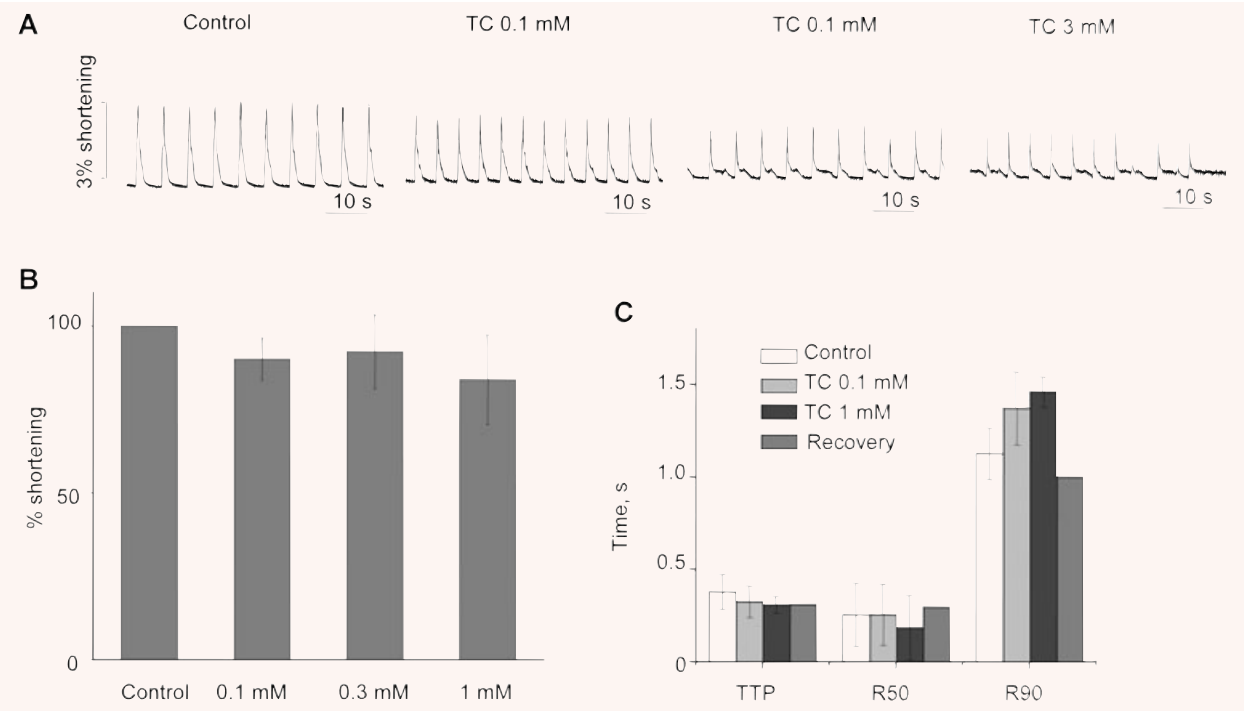

Fig. 9 (**A**) Example trace for contraction of human adult cardiomyocytes in 0.1, 1 and 3 mM TC. (**B**) Effect of TC on % of shortening of human adult cardiomyocytes: 3 mM concentration is not shown because of the disruption of rate at this concentration. (**C**) Effect of TC on times to peak contraction (TTP) and to 50% and 90% relaxation (R50 and R90) in human adult cardiomyocytes.

relatively well maintained. Development of sarcoplasmic reticulum (SR) calcium store contribution to excitation–contraction coupling, a hallmark of the adult phenotype, has been observed in hESC-CM culture [38], but there are differences between groups in whether and when this occurs [38, 39]. SR contribution is characterized by appearance of the key SR proteins such as RyR, phospholamban and SERCA2a, and by sensitivity to SR Ca-channel opener caffeine and the SERCA2a inhibitor, thapsigargin. Characteristically, the maturation time for hESC-CM is longer than that for mESC-CM, though it should be noted that the maximum time in culture for hESC-CM is being continually extended: we have observed these cells to 7 months [12]. In terms of the present work, our definitions of early and late mouse and human ESC-CM are approximately consistent with the available literature on the various markers of maturity.

The observations reported in this study are consistent with our results using neonatal and adult rat cardiomyocytes that indicated that the bile acid arrhythmias are Ca^{2+} related. Our results using cardiomyocytes are similar to data demonstrating that bile acids increase the intracellular calcium concentration in vascular endothelial cells [40]. We have shown here that TC-induced intracellular calcium release is associated with desynchronization of ES–derived cardiomyocyte networks. We previously postulated that the Ca^{2+} disturbance could arise *via* the membrane, with effects on Ca^{2+} related currents, Na^{+}/Ca^{2+} exchange currents, or bile acid-Na^{+} exchange currents [25]. It is interesting to note that the effects of TC on the immature ESC-CM were not only more potent but more difficult to reverse by washing. Whether this represents an irreversible change in ion channel conformation or an effect of calcium overload to damage the myocyte is unknown. One notable aspect of the present study is that the use of the SICM allows identification and tracking of contraction and calcium transients of ESC-CM even within a mixed population of other cell types, as we have previously described [30]. In summary we demonstrate that less mature murine and human ESCM are more susceptible to bile acid-induced arrhythmias, and that this is lost as the maturity of the phenotype progresses. The use of hESC-CM in particular opens the possibility not only for definition of mechanisms and testing of potential therapeutic agents, but for defining the genetic and epigenetic contributions to the susceptibility of some pregnancies to choleostatic intrauterine fetal death.

Acknowledgements

Research was supported by Action Medical Research, NC3R, Universiti Teknologi Mara in Malaysia, Geron Corporation and Clinical Research Committee (CRC) of Royal Brompton and Harefield.

Supporting Information

Additional Supporting Information may be found in the online version of this article.

Movie S1. Ca^{2+} dynamics of mESC-CM loaded with Fluo-4 after addition of 1.0 mM TC.

Movie S2. Ca^{2+} dynamics of hESC-CM loaded with Fluo-4 after addition of 1.0 mM TC.

This material is available as part of the online article from: http://www.blackwell-synergy.com/doi/abs/10.1111/j.1582-4934.2009.00741.x
(This link will take you to the article abstract).

Please note: Wiley-Blackwell are not responsible for the content or functionality of any supporting materials supplied by the authors. Any queries (other than missing material) should be directed to the corresponding author for the article.

References

1. **Hescheler J, Fleischmann BK, Lentini S, *et al.*** Embryonic stem cells: a model to study structural and functional properties in cardiomyogenesis. *Cardiovasc Res*. 1997; 2: 149–62.
2. **Kehat I, Kenyagin-Karsenti D, Snir M, *et al.*** Human embryonic stem cells can differentiate into myocytes with structural and functional properties of cardiomyocytes. *J Clin Sci*. 2001; 108: 407–14.
3. **Brito-Martins M, Harding SE, Ali NN**. [beta]1- and [beta]2-adrenoceptor responses in cardiomyocytes derived from human embryonic stem cells: comparison with failing and non-failing adult human heart. *Br J Pharmacol*. 2008; 153: 751–9.
4. **Xu C, Police S, Rao N, *et al.*** Characterization and enrichment of cardiomyocytes derived from human embryonic stem cells. *Circ Res*. 2002; 91: 501–8.
5. **Mummery C, Ward-van Oostwaard D, Doevendans P, *et al.*** Differentiation of human embryonic stem cells to cardiomyocytes: role of coculture with visceral endoderm-like cells. *Circulation*. 2003; 107: 2733–40.
6. **Klug MG, Soonpaa MH, Koh GY, *et al.*** Genetically selected cardiomyocytes from differentiating cells form stable intracardiac grafts. *J Clin Invest*. 1996; 98: 216–24.
7. **Laflamme MA, Chen KY, Naumova AV, *et al.*** Cardiomyocytes derived from human embryonic stem cells in pro-survival factors enhance function of infarcted rat hearts. *Nat Biotech*. 2007; 25: 1015–24.
8. **Scolding N, Marks D, Rice C.** Autologous mesenchymal bone marrow stem cells: practical considerations. *J Neurol Sci*. 2008; 265: 111–5.
9. **van Laake LW, Hassink R, Doevendans PA, *et al.*** Heart repair and stem cells. *J Physiol*. 2006; 577: 467–78.
10. **Louch WE, Bito V, Heinzel FR, *et al.*** Reduced synchrony of Ca2+ release with loss of T-tubules-a comparison to Ca2+ release in human failing cardiomyocytes. *Cardiovasc Res*. 2004; 62: 63–73.
11. **Piper HM, Jacobson SL, Schwartz P.** Determinants of cardiomyocyte development in long-term primary culture. *J Mol Cell Cardiol*. 1988; 20: 825–35.
12. **Harding SE, Ali NN, Brito-Martins M, *et al.*** The human embryonic stem cell-derived cardiomyocyte as a pharmacological model. *Pharmacol Ther*. 2007; 113: 341–53.
13. **Sartiani L, Bettiol E, Stillitano F, *et al.*** Developmental changes in cardiomyocytes differentiated from human embryonic stem cells: a molecular and electrophysiological approach. *Stem Cells*. 2007; 25: 1136–44.
14. **Fisk NM, Storey GN.** Fetal outcome in obstetric cholestasis. *Br J Obstet Gynaecol*. 1988; 95: 1137–43.
15. **Reid R, Ivey KJ, Rencoret RH, *et al.*** Fetal complications of obstetric cholestasis. *Br Med J*. 1976; 1: 870–2.
16. **Rioseco AJ, Ivankovic MB, Manzur A, *et al.*** Intrahepatic cholestasis of pregnancy: a retrospective case-control study of perinatal outcome. *Am J Obstet Gynecol*. 1994; 170: 890–5.
17. **Abedin P, Weaver JB, Egginton E.** Intrahepatic cholestasis of pregnancy: prevalence and ethnic distribution. *Ethn Health*. 1999; 4: 35–7.
18. **Gerloff T, Stieger B, Hagenbuch B, *et al.*** The sister of P-glycoprotein represents the canalicular bile salt export pump of mammalian liver. *J Biol Chem*. 1998; 273: 10046–50.
19. **Costoya AL, Leontic EA, Rosenberg HG, *et al.*** Morphological study of placental terminal villi in intrahepatic cholestasis of pregnancy: histochemistry, light and electron microscopy. *Placenta*. 1980; 1: 361–8.
20. **Laatikainen T, Tulenheimo A.** Maternal serum bile acid levels and fetal distress in cholestasis of pregnancy. *Int J Gynaecol Obstet*. 1984; 22: 91–4.
21. **Laatikainen TJ**. Fetal bile acid levels in pregnancies complicated by maternal intrahepatic cholestasis. *Am J Obstet Gynecol*. 1975; 122: 852–6.
22. **Kramer W, Buscher HP, Gerok W, *et al.*** Bile salt binding to serum components. Taurocholate incorporation into high-density lipoprotein revealed by photoaffinity labelling. *Eur J Biochem*. 1979; 102: 1–9.
23. **Sant'Anna AM, Fouron JC, Alvarez F**. Neonatal cholestasis associated with fetal arrhythmia. *J Pediatr*. 2005; 146: 277–80.
24. **Glantz A, Marschall HU, Mattsson LA**. Intrahepatic cholestasis of pregnancy: Relationships between bile acid levels and fetal complication rates. *Hepatology*. 2004; 40: 467–74.
25. **Gorelik J, Harding SE, Shevchuk AI, *et al.*** Taurocholate induces changes in rat cardiomyocyte contraction and calcium dynamics. *Clin Sci*. 2002; 103: 191–200.
26. **Williamson C, Gorelik J, Eaton BM, *et al.*** The bile acid taurocholate impairs rat cardiomyocyte function: a proposed mechanism for intra-uterine fetal death in obstetric cholestasis. *Clin Sci*. 2001; 100: 363–9.
27. **Boheler KR, Czyz J, Tweedie D, *et al.*** Differentiation of pluripotent embryonic stem cells into cardiomyocytes. *Circ Res*. 2002; 91: 189–201.
28. **Harding SE, Vescovo G, Kirby M, *et al.*** Contractile responses of isolated adult rat and rabbit cardiac myocytes to isoproterenol and calcium. *J Mol Cell Cardiol*. 1988; 20: 635–47.
29. **Korchev YE, Bashford CL, Milovanovic M, *et al.*** Scanning ion conductance microscopy of living cells. *Biophys J*.1997; 73: 653–8.
30. **Gorelik J, Ali NN, Shevchuk AI, *et al.*** Functional characterization of embryonic stem cell-derived cardiomyocytes using

scanning ion conductance microscopy. *Tissue Eng*. 2006; 12: 657–64.

31. **Shevchuk AI, Gorelik J, Harding SE, *et al.*** Simultaneous measurement of Ca^{2+} and cellular dynamics: combined scanning ion conductance and optical microscopy to study contracting cardiac myocytes. *Biophys J*. 2001, 81: 1759–64.
32. **Lopez JR, Jovanovic A, Terzic A**. Spontaneous calcium waves without contraction in cardiac myocytes. *Biochem Biophys Res Commun*. 1995; 214: 781–7.
33. **Yuasa S, Itabashi Y, Koshimizu U, *et al.*** Transient inhibition of BMP signaling by Noggin induces cardiomyocyte differentiation of mouse embryonic stem cells. *Nat Biotech*. 2005; 23: 607–11.
34. **Yamashita JK, Takano M, Hiraoka-Kanie M, *et al.*** Prospective identification of cardiac progenitors by a novel single cell-based cardiomyocyte induction. *FASEB J*. 2005; 19: 1534–6.
35. **Al Inizi S, Gupta R, Gale A**. Fetal tachyarrhythmia with atrial flutter in obstetric cholestasis. *Int J Gynaecol Obstet*. 2006; 93: 53–4.
36. **Snir M, Kehat I, Gepstein A, *et al.*** Assessment of the ultrastructural and proliferative properties of human embryonic stem cell-derived cardiomyocytes. *Am J Physiol Heart Circ Physiol*. 2003; 285: H2355–63.
37. **Engel FB, Schebesta M, Duong MT, *et al.*** p38 MAP kinase inhibition enables proliferation of adult mammalian cardiomyocytes. *Genes Dev*. 2005; 19: 1175–87.
38. **Liu J, Fu JD, Siu CW, *et al.*** Functional sarcoplasmic reticulum for calcium handling of human embryonic stem cell-derived cardiomyocytes: insights for driven maturation. *Stem Cells*. 2007; 25: 3038–44.
39. **Dolnikov K, Shilkrut M, Zeevi-Levin N, *et al.*** Functional properties of human embryonic stem cell-derived cardiomyocytes: intracellular Ca2+ handling and the role of sarcoplasmic reticulum in the contraction. *Stem Cells*. 2006; 24: 236–45.
40. **Nakajima T, Okuda Y, Chisaki K, *et al.*** Bile acids increase intracellular Ca(2+) concentration and nitric oxide production in vascular endothelial cells. *Br J Pharmacol*. 2000; 130: 1457–67.